PNAS RESEARCH ARTICLE | BIOPHYSICS AND COMPUTATIONAL BIOLOGY BIOCHEMISTRY OPEN ACCESS

Assignment of structural transitions during mechanical unwrapping of nucleosomes and their disassembly products

César Díaz-Celis[a,b,c,1], Cristhian Cañari-Chumpitaz[a,b,c,d,1], Robert P. Sosa[a,b,e,1], Juan P. Castillo[a,b,1,2], Meng Zhang[b,f,g], Enze Cheng[a,b,h], Andy Q. Chen[i], Michael Vien[i], JeongHoon Kim[a,b], Bibiana Onoa[a,b,c], and Carlos Bustamante[a,b,c,d,h,i,j,k,l,3]

Contributed by Carlos Bustamante; received April 13, 2022; accepted June 7, 2022; reviewed by Douglas Smith and Bin Zhang

Nucleosome DNA unwrapping and its disassembly into hexasomes and tetrasomes is necessary for genomic access and plays an important role in transcription regulation. Previous single-molecule mechanical nucleosome unwrapping revealed a low- and a high-force transitions, and force-FRET pulling experiments showed that DNA unwrapping is asymmetric, occurring always first from one side before the other. However, the assignment of DNA segments involved in these transitions remains controversial. Here, using high-resolution optical tweezers with simultaneous single-molecule FRET detection, we show that the low-force transition corresponds to the undoing of the outer wrap of one side of the nucleosome (~27 bp), a process that can occur either cooperatively or noncooperatively, whereas the high-force transition corresponds to the simultaneous unwrapping of ~76 bp from both sides. This process may give rise stochastically to the disassembly of nucleosomes into hexasomes and tetrasomes whose unwrapping/rewrapping trajectories we establish. In contrast, nucleosome rewrapping does not exhibit asymmetry. To rationalize all previous nucleosome unwrapping experiments, it is necessary to invoke that mechanical unwrapping involves two nucleosome reorientations: one that contributes to the change in extension at the low-force transition and another that coincides but does not contribute to the high-force transition.

nucleosome | nucleosome unwrapping | nucleosome disassembly | optical trapping | FRET

Significance

Nucleosomes, the fundamental structural unit of chromatin, consists of ~147 DNA base pairs wrapped around a histone protein octamer. To characterize the strength of the nucleosomal barrier and its contribution as a mechanism of control of gene expression, it is essential to determine the forces required to unwrap the DNA from the core particle and the stepwise transitions involved. In this study, we performed combined optical tweezers and single-molecule fluorescence measurements to identify the specific DNA segments unwrapped during the force transitions observed in mechanical stretching of nucleosomes. Furthermore, we characterize the mechanical signatures of subnucleosomal hexasomes and tetrasomes. The characterization performed in this work is essential for the interpretation of ongoing studies of chromatin remodelers, polymerases, and histone chaperones.

Chromatin is a nucleoprotein complex that regulates DNA accessibility for replication, repair, and transcription in eukaryotic cells. The structural unit of chromatin is the nucleosome, which consists of 147 bp of DNA wrapped in 1.65 left-handed turns around an octamer of histone proteins (1, 2). The octamer core is composed of two copies each of histones H2A, H2B, H3, and H4, organized in two H2A-H2B heterodimers and in one $(H3\text{-}H4)_2$ tetramer. The histone core is stabilized mainly by hydrophobic attractions, while DNA-histone contacts involve hydrogen bonds and electrostatic interactions (2). Nucleosomes are highly dynamic and intrinsically plastic complexes which are subject to extensive modifications to regulate access to DNA, including exchange of canonical histones with histone variants, histone posttranslational modifications, and interactions with regulatory proteins such as histone chaperones and molecular motors (RNA polymerase, remodelers, etc.). These modifications alter histone-DNA interactions, leading to nucleosome disassembly into subnucleosomal particles—hexasomes and tetrasomes—and the exposure of DNA (3–8). Accordingly, a detailed picture of nucleosomal regulation of gene expression requires a precise characterization of the mechanical stability of the nucleosome and how fluctuations, forces, and torques affect its integrity.

The binding of DNA to the histone core and the structural transitions that occur during nucleosome disassembly have traditionally been studied by bulk approaches (9–13). An alternative approach is the use of single-molecule mechanical manipulation with optical or magnetic trapping. These methods provide insight into the process by which the cellular machinery access the nucleosome-bound DNA and the effect of epigenetics modifications on nucleosome accessibility. These experiments include the mechanical stretching of chromatin fibers and nucleosome arrays (14–20) and of single nucleosomes (21–24). Likewise, torque has been applied to nucleosomes using magnetic trapping (25, 26) and torsional optical tweezers (27).

These single-molecule force-extension experiments revealed that under applied force, DNA unwraps from the histone core in two stages. The first, occurring between 3 and 6 pN, was assigned to the unwrapping of the outer DNA turn, releasing 60 to 70 bp in a reversible manner. The second, taking place over a broad range of forces (8 to 40 pN), is characterized by an abrupt change in extension or rip and was attributed to the unwrapping of the DNA inner turn (~80 bp) (16, 17, 21, 23, 24, 27). Even though the estimated amount of unwrapped DNA described in these studies was in agreement with the

Reviewers: D.S., University of California, San Diego, and B.Z., Massachusetts Institute of Technology.

The authors declare no competing interest.

[1]C.D.-C., C.C.-C., R.P.S., and J.P.C. contributed equally to this work.

[2]Present address: Soft Matter and Technology Center, Departamento de Física, Facultad de Ciencia, Universidad de Santiago, Santiago, 9170022, Chile.

[3]To whom correspondence may be addressed. Email: carlosjbustamante2@gmail.com.

This article contains supporting information online at http://www.pnas.org/lookup/suppl/doi:10.1073/pnas.2206513119/-/DCSupplemental.

Published August 8, 2022.

nucleosome crystal structure, these experiments assumed that unwrapping under tension occurs symmetrically from both ends of the nucleosome.

In contrast, combined single-molecule fluorescence-force spectroscopy experiments of fluorescence resonance energy transfer (FRET) pair-labeled nucleosomes revealed that the low-force transition corresponds only to the unwrapping of one outer-wrap DNA arm, whereas the high-force transition corresponded to the unidirectional unwrapping of internal nucleosome positions and the other arm. Thus, according to these studies, DNA unwrapping under tension is asymmetric and occurs from the weak toward the strong arm (22). Although these single-molecule fluorescence experiments targeted specific regions of nucleosomal DNA, they were not able to directly measure the changes in extension associated with each force transition due to limited resolution. Taken together, the interpretation of the changes in extension observed by previous pulling experiments remain inconclusive. Likewise, the force-extension mechanical signatures of hexasomes and tetrasomes have not been established.

Here we use high-resolution optical tweezers with single-molecule fluorescence detection capability (fleezers) to characterize the unwrapping and rewrapping of nucleosomes, hexasomes, and tetrasomes under tension. We assign each force transition to the unwrapping of specific DNA regions, monitor the integrity of nucleosomes during their mechanical unwrapping, and find that their disassembly is stochastic. Our results reconcile previous discrepancies in the interpretation of single-molecule mechanical unwrapping of nucleosomes.

Results

Mechanical Signatures of Nucleosome Unwrapping. We assembled nucleosomes by salt dialysis, using a recombinant *Xenopus laevis* histone core and the artificial 601 nucleosome-positioning sequence (NPS), and purified them using polyacrylamide gel electrophoresis (Fig. 1*A*). To perform the mechanical unwrapping experiments, nucleosomes were anchored to microbeads that were trapped in the high-resolution optical tweezers instrument (Fig. 1*B*).

At low ionic strength (50 mM KOAc), pulling curves showed the two force-extension transitions previously described for single nucleosomes at low and at high forces (21, 23) (Fig. 1*C* and *SI Appendix*, Table S1). In our conditions, the low-force transition ($N = 53$) manifests as 1) a noncooperative transition at 3.9 ± 0.3 pN that is observed in the majority of the pulling curves (87%; $n = 46$) and that appears as a shoulder or plateau in the force-extension curve, with an extension of ∼19 nm (Fig. 1 *C*, *Left*); 2) a cooperative transition at 4.1 ± 0.7 pN (9%; $n = 5$), characterized by an abrupt change in extension or rip of 20.4 ± 1.5 nm (Fig. 1 *C*, *Middle*); or 3) a combination of the cooperative and noncooperative transitions at 3.8 ± 0.2 pN (4%; $n = 2$), with a change in extension of 20.6 ± 2.0 nm (Fig. 1 *C*, *Right*).

In previous studies using reconstituted chicken erythrocyte nucleosomes, the low-force transition at 50 mM KOAc (21) and at 10 mM NaN_3 (23) appeared as a rip and became progressively less cooperative as the ionic strength was increased to 200 mM KOAc (21). To determine if the ionic strength modifies the unwrapping trajectory of the low-force transition, we stretched nucleosomes at a lower (∼10 mM K^+ from KOH) and at a higher (200 mM KOAc) concentration (*SI Appendix*, Fig. S1 *A* and *B* and Table S1). We observed no change in the frequency (>85%) or the extension of the noncooperative transition with the increased ionic strength, while the force decreases slightly (*SI Appendix*, Table S1).

Because nucleosome stability depends on the DNA sequence, we analyzed the low-force transition of *X. laevis* nucleosomes assembled on the natural 5S rRNA NPS, which unlike the artificial 601 NPS (28, 29), has a lower affinity for the octamer, resulting in less accurate positioning and stability (30). In 50 mM KOAc, 98% of the low-force transitions of the 5S nucleosomes are noncooperative (*SI Appendix*, Fig. S1*C* and Table S1), indicating that the

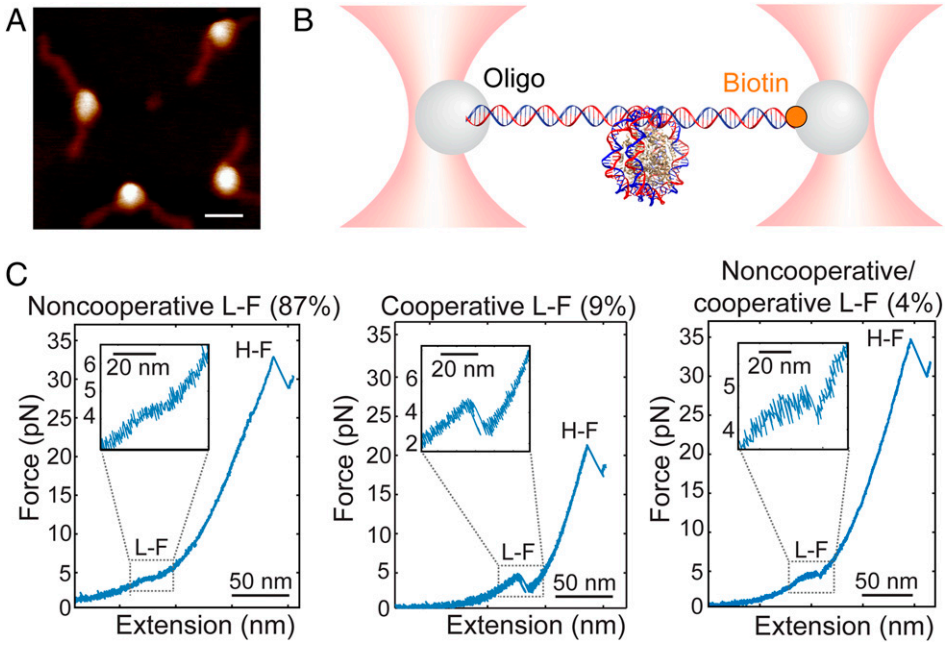

Fig. 1. Nucleosome unwrapping trajectory under tension. (*A*) AFM of purified *X. laevis* 601 nucleosomes (average maximum height ∼3.9 nm, $n = 4$; scale bar, 20 nm). (*B*) Experimental geometry for single nucleosome manipulation using high-resolution optical tweezers. The nucleosome was ligated to DNA handles, which were then tethered to 1-μm polystyrene microbeads by ligation to DNA oligo-coated beads and by biotin binding to streptavidin-coated beads. (*C*) Examples of force-extension unwrapping trajectories of single nucleosomes. The low-force transition (L-F) can be noncooperative (*Left*), cooperative (*Middle*), or a combination of both mechanisms (*Right*). The high-force transition (H-F) is distinguished by a rip.

NPS has a small effect on the low-force unwrapping trajectories. Likewise, the low-force transition is not dependent on the recombinant nucleosome source [*X. laevis*, human (*SI Appendix*, Fig. S2*A*), or yeast (*SI Appendix*, Fig. S2*B* and Table S1)].

The second force-extension transition of nucleosome unwrapping is characterized by a rip that occurs abruptly over a broad range of forces above ∼12 pN up to ∼37 pN (Fig. 1*C* and *SI Appendix*, Table S2). At 50 mM KOAc, the high-force transition occurs at 30.4 ± 8.3 pN—higher than the corresponding transition observed with nucleosomes assembled with native histones (21)—and exhibits a change in extension of 24.5 ± 1.6 nm. The ionic strength does not affect the cooperativity of this transition or the change in extension (*SI Appendix*, Table S2); at 10 mM K^+ from KOH, the high-force rip is centered at ∼35 pN (*SI Appendix*, Fig. S1*A* and Table S2), while at 200 mM KOAc, the high-force rip occurs at ∼24 pN (*SI Appendix*, Fig. S1*B* and Table S2). The reduction of the unwrapping force with ionic strength agrees with the electrostatic nature of DNA-histone interactions. In the case of *X. laevis* 5S (*SI Appendix*, Fig. S1*C*) and human 601 nucleosomes (*SI Appendix*, Fig. S2*A*), the high-force transition at 50 mM KOAc is seen at ∼29 pN, while for yeast 601 nucleosomes, it occurs at ∼21 pN (*SI Appendix*, Fig. S2*B*). These observations suggest different histone-DNA interactions between recombinant nucleosomes from vertebrates and invertebrates. Despite these differences in force, the change in extension is similar for all three types of recombinant nucleosomes (*SI Appendix*, Table S2).

To summarize, the majority of trajectories of recombinant nucleosomes displayed a noncooperative low-force transition and a high-force rip centered at high forces, in contrast to those of nucleosomes assembled with native histones, which are characterized by a cooperative low-force transition and a high-force rip below ∼15 pN (21, 31). These discrepancies may be due to the presence of posttranslational modifications in the native octamers, some of which have been shown to affect the mechanical unwrapping of nucleosome arrays (16, 19).

Mechanical Unwrapping of Nucleosomes Generates Hexasomes and Tetrasomes. In vitro studies have shown that nucleosome destabilization at increasing concentrations of salt proceeds via DNA unwrapping and the sequential dissociation of H2A-H2B heterodimers, yielding hexasomes and tetrasomes (9–13, 32). However, these intermediates have not been identified in mechanical disassembly experiments, nor have their unwrapping trajectories been characterized.

To investigate the disassembly of nucleosomes under force, we subjected nucleosomes to successive pulling/relaxation cycles, from low to high force and back, until we obtained the force-extension curve of bare DNA, indicating full disassembly. The first pulling curve (Fig. 2*A*) represents the intact nucleosome and shows the two force-extension transitions previously described. The second and third cycles display two distinct types of unwrapping trajectories with a single force-extension signature each. The first type of trajectory (Fig. 2 *A*, type I) exhibits a rip or cooperative transition centered at 23.8 ± 4.3 pN ($n = 42$), with a change in extension of 23.4 ± 1.1 nm. The second or type II trajectory typically precedes the bare DNA force-extension signature and exhibits a transition at low force (4.5 ± 0.8 pN; $n = 40$), a net change in extension of 14.9 ± 1.7 nm, and a plateau shape that displayed dynamic fluctuations (hopping). Disassembly of *X. laevis* 5S nucleosomes, as well as human and yeast 601 nucleosomes, also produces type I and type II pulling trajectories (*SI Appendix*, Fig. S3 *A*–*C*).

To establish the identity of the type I and type II pulling trajectories, we purified hexasomes and tetrasomes and characterized them by atomic force microscopy (AFM) (*SI Appendix*, Fig. S4 *A* and *B*). The first pulling curve of hexasomes (Fig. 2*B*) showed an unwrapping trajectory indistinguishable from the type I trajectory, displaying a single rip of 23.4 ± 1.1 nm at a force of 24.6 ± 3.0 pN. Successive pulling/relaxation cycles of hexasomes also generate type II and bare DNA trajectories, in that order. Force-extension trajectories of tetrasomes (Fig. 2*C*) exhibit a single transition of 13.3 ± 1.7 nm at a force of 4.4 ± 0.5 pN, resembling the type II trajectories. Interestingly, pulling trajectories of nucleosomes, hexasomes, and tetrasomes were not always observed consecutively through pulling/relaxation cycles (Fig. 2*A*): a nucleosome can also disassemble directly into tetrasomes or bare DNA with different probabilities depending on the ionic strength (Fig. 2*D* and *SI Appendix*, Table S3),

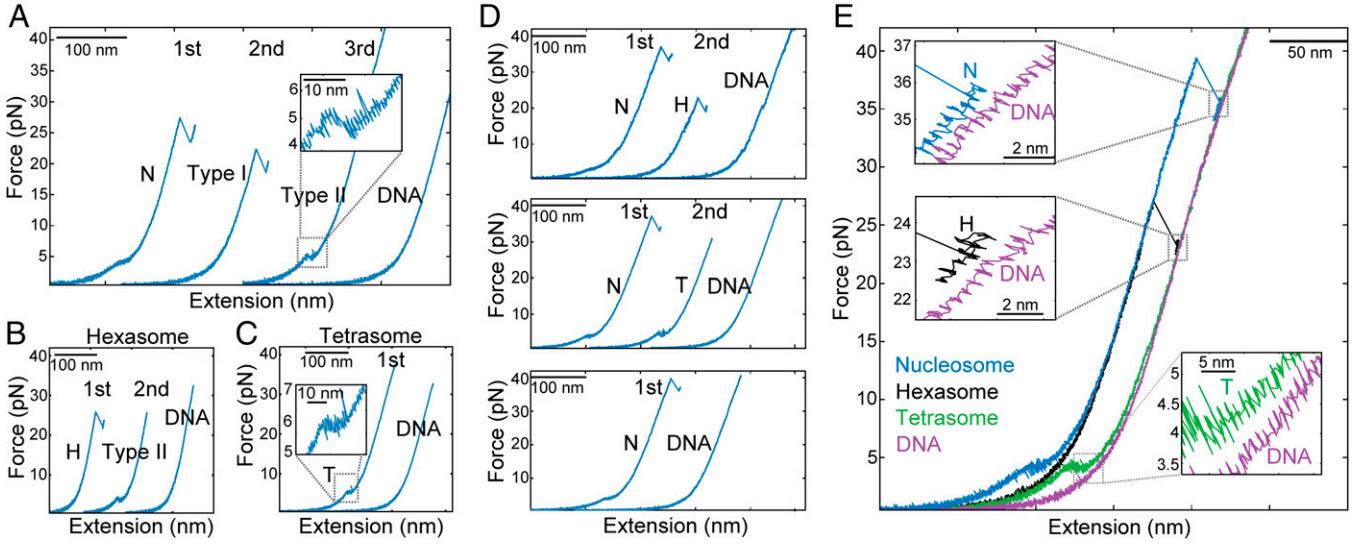

Fig. 2. Nucleosome (N) disassembly under force generates hexasomes (Hs) and tetrasomes (Ts) and is stochastic. (*A*) N disassembly by pulling and relaxation cycles (first, second, and third) at 50 mM KOAc. Only pulling curves (blue) are shown, and they were arbitrarily shifted along the horizontal axis for illustrative purposes. (*A*) The first pulling curve corresponds to the N. Type I and type II intermediates were observed in the pulling curves of the second and third cycles, respectively. (*B*) H disassembly. Type II intermediate was generated in the second cycle. (*C*) T disassembly. (*D*) Under force, Ns can disassemble into H without forming Ts before full dissociation (*Top*), disassemble into T (*Middle*), or fully dissociate in one pulling and relaxation cycle (*Bottom*). (*E*) Unwrapping trajectories of Ns, Hs, Ts, and DNA.

indicating that the mechanical disassembly is stochastic. Fig. 2*E* depicts the characteristic force-extension curves of nucleosomes, hexasomes, tetrasomes, and bare DNA. Notice that after the last unwrapping transition (insets), the pulling curve of bare DNA is longer by 2.3 ± 0.6 nm (n = 20), 2.5 ± 0.8 nm (n = 14), and 7.8 ± 1.7 nm (n = 17) than those of the nucleosome, hexasome, and tetrasome, respectively, indicating that even at forces > 30 pN, part of the DNA remains wrapped around the histone core.

Previous stretching experiments using torsional optical tweezers of tetrasomes assembled with $(H3\text{-}H4)_2$ tetramers reported pulling curves displaying a single rip at ∼16 pN (27), resembling those of hexasomes described here (Fig. 2*B*) and quite different from the pulling curves of tetrasomes characterized also in this study (Fig. 2*C*). We proposed that this discrepancy results from $(H3\text{-}H4)_2$ tetramer oligomerization into nucleosome-like particles as previously described (33–35). Indeed, using AFM, we found that whereas at a 1:1.4 $(H3\text{-}H4)_2$:DNA ratio, $(H3\text{-}H4)_2$ tetramers form mainly tetrasomes, at higher $(H3\text{-}H4)_2$:DNA ratios (1:2.6), they assemble into bigger particles resembling hexasomes and nucleosomes (*SI Appendix*, Fig. S4*C*). Moreover, we determined that the unwrapping trajectories of these bigger $(H3\text{-}H4)_2$ oligomers resemble those of purified hexasomes and exhibit a change in extension of 24.5 ± 1.5 nm centered at 16.9 ± 3.8 pN (n = 14) (*SI Appendix*, Fig. S4 *D* and *E*).

Nucleosome, Hexasome, and Tetrasome Rewrapping Trajectories. Unwrapping trajectories of nucleosomes were observed in successive pulling curves during disassembly experiments, indicating that during relaxation, full rewrapping had taken place (Fig. 3*A*). These nucleosome rewrapping events occur in a solution free of histones; therefore, the observations of rewrapping imply that histones must have remained bound to the DNA after unwrapping. The relaxation curves following the first pulling of nucleosomes

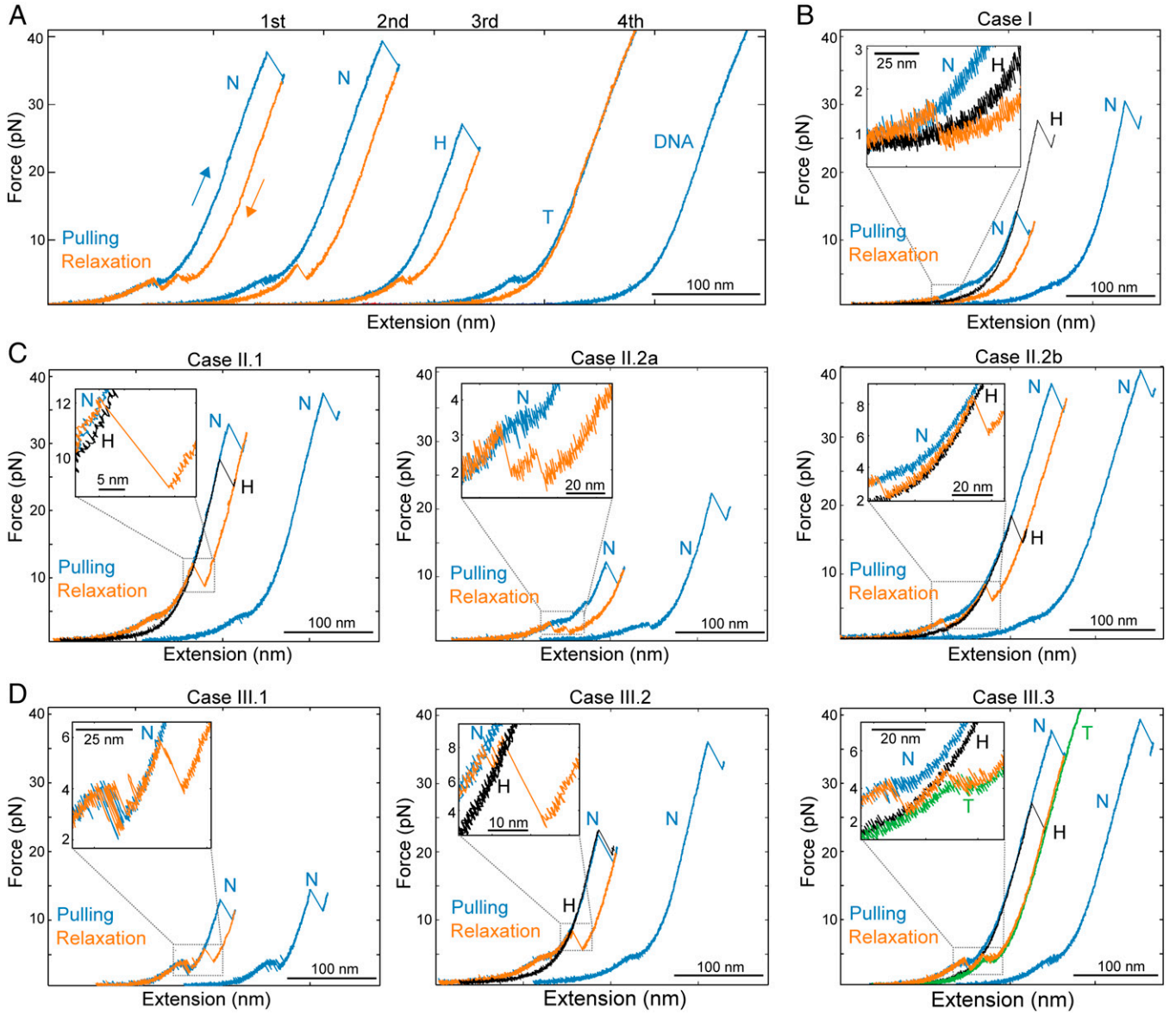

Fig. 3. Reversible assembly of Ns. (*A*) N disassembly at 50 mM KOAc after four cycles of pulling and relaxation. Pulling/relaxation cycles were arbitrarily shifted along the horizontal axis for clarity. The second pulling corresponds to the unwrapping trajectory of a N, which indicates N rewrapping during the first relaxation. H and T trajectories were observed in the pulling curves of the third and fourth cycles, respectively. (*B*) N rewrapping via a single zip (case I). The H pulling curve (black curve) was superposed to identify the formation of intermediates. (*C*) Three types (cases II.1, II.2a, and II2.b) of N rewrapping via two shortening transitions. H unwrapping trajectories are in black. (*D*) Three types (cases III.1, III.2, and III.3) of N rewrapping via three shortening transitions. In case III.3, the T (green curve) and H (black curve) unwrapping trajectories were superposed to identify the rewrapping of intermediates.

are identified as nucleosome rewrapping trajectories only if the subsequent pulling curve displays the low- and high-force transitions. The relaxation trajectories can show one (Fig. 3*B*), two (Fig. 3*C*), or three (Fig. 3*D*) shortening transitions over a broad range of forces (2 to 15 pN). Having characterized the unwrapping trajectories of tetrasomes and hexasomes, we were able to interpret and assign the relaxation transitions to the rewrapping of specific nucleosomal intermediates.

The single shortening transition occurs at a force below the low-force unwrapping transition (Fig. 3*B*). It is a cooperative rewrapping event and shows a decrease in extension of ∼40 nm, corresponding to the rewrapping at once of the DNA unwrapped during the previous low- and high-force transitions (case I). The term "zip" is henceforth used to describe this type of sudden, cooperative transition. When the relaxation curve displays two shortening transitions, there are three cases. In the first case (case II.1), one of the transitions is a zip that occurs at a force higher than the low-force unwrapping transition (Fig. 3 *C*, *Left*); in this case, the rewrapping trajectory reaches the partially unwrapped nucleosome pulling curve and is continued by a second noncooperative shortening transition that follows the pulling curve all the way to zero force, resulting in a fully wrapped nucleosome. The zip exhibits a decrease in extension of ∼22 nm, indicating that it corresponds to the rewrapping of the DNA unwrapped during the previous high-force rip. In the second case (case II.2), the relaxation curve displays two zips; these can be of variable size and may occur with both below (case II.2a; Fig. 3 *C*, *Middle*) or one above and one below (case II.2b; Fig. 3 *C*, *Right*) the low-force unwrapping transition. In these cases, the first zip corresponds to the rewrapping of the hexasome, whereas the second zip corresponds to the full rewrapping of the nucleosome. When the relaxation curve displays three shortening transitions, there are three cases. In the first case (case III.1), the relaxation curves display two zips below or near the low-force unwrapping transition, followed by noncooperative shortening (Fig. 3 *D*, *Left*). In the second case (case III.2), the relaxation curves display two zips above the low-force unwrapping transition, followed by noncooperative shortening (Fig. 3 *D*, *Middle*). In both of these cases, the first zip, as before, reaches the hexasome pulling trajectory, and the second corresponds to the formation of the partially unwrapped nucleosome, followed by the full rewrapping of the nucleosome via the noncooperative transition. In the third case (case III.3), the first transition is noncooperative, occurs at a force close to the noncooperative unwrapping transition, and overlaps with the tetrasome unwrapping trajectory; it is followed by two zips of variable size, the first of which reaches the hexasome pulling trajectory and the second of which represents the formation of the fully wrapped nucleosome (Fig. 3 *D*, *Right*). Accordingly, nucleosome rewrapping can occur via sequential rewrapping around tetrasomes and hexasomes, through hexasomes alone, or in a single or two steps without detectable intermediates.

A similar analysis has been performed for the rewrapping of hexasomes (*SI Appendix*, Fig. S5*A*) and tetrasomes (*SI Appendix*, Fig. S5*B*) during nucleosome disassembly. Interestingly, in a few cases, tetrasomes that have been generated by nucleosome disassembly in which the pulling and relaxation cycles did not exceed ∼10 pN by design, we observed pulling curves going back to those characteristics of the unwrapping of hexasomes, displaying a single rip at high force (*SI Appendix*, Fig. S5*C*). One possible explanation for this observation is that the H2A-H2B heterodimer remained bound to the DNA during unwrapping and eventually re-engaged the tetrasome to reform a hexasome.

Annotation of Mechanically Induced Transitions by Simultaneous Detection of Force and FRET Signals. Ngo et al. (22) used single-molecule FRET experiments of nucleosomes labeled at different positions of the 601 NPS to show that under tension, unwrapping is asymmetric and its directionality is dictated by sequence-dependent DNA flexibility. These authors showed that unwrapping begins at low force with the less flexible DNA arm (monitored by a FRET pair labeled ED1), followed by an internal position opposite to the dyad at higher force (monitored by a FRET pair labeled INT) and ending with the unwrapping of the more flexible arm (monitored by FRET pair ED2).

In order to unambiguously assign the force-extension transitions of nucleosome unwrapping with the specific DNA segments involved, we used fleezers (36–38). To that end, we synthetized and purified ED1, INT, and ED2 nucleosomes (labeled with Cy3/Cy5 pairs) (Fig. 4*A*), which were ligated to 2.5-kb DNA handles to allow their attachment to functionalized polystyrene microbeads (Fig. 4*B*). We first confirmed the presence of both dyes and the FRET state corresponding to a fully wrapped nucleosome using the confocal scan of the instrument (Fig. 4*C*). Next, we monitored the cotemporal evolution of force, extension, and fluorescence of individual fluorophores and FRET of ED2 (Fig. 4*D*), INT (*SI Appendix*, Fig. S6*A*), and ED1 (*SI Appendix*, Fig. S6*B*) during pulling and relaxation cycles. We used a symmetric pulling protocol in which both optical traps were moved simultaneously in order to keep the fluorescently labeled nucleosome at the center of the confocal spot. The fluorescence channel shows the anticorrelated changes of Cy5 and Cy3 fluorescence with the corresponding high-to-low and low-to-high FRET transitions during the unwrapping and rewrapping trajectories, respectively. The recovery of FRET in the rewrapping rules out photobleaching of the acceptor dye during the experiments.

Detailed comparison of the time course between force-extension and FRET signals of all molecules tested indicates that within our temporal resolution (10 ms) for both ED2 (Fig. 5 *A* and *B*) and INT (Fig. 5 *C* and *D*) nucleosomes, the FRET change occurs simultaneously with the force-extension transition at high force, regardless of whether the low-force transition was cooperative or noncooperative (Fig. 5 *A* and *C*, *Left* and *Right*, respectively). We noted that prior to the transition, the INT nucleosome exhibits larger fluctuations in FRET compared to the ED2 nucleosome, a behavior previously described as gaping (39). The simultaneous decay of FRET with the high-force rip implies that the changes in end-to-end distance (measured by optical tweezers) and the local DNA changes (as monitored by FRET) are caused by the same DNA unwrapping process.

In contrast, for ED1 nucleosomes, we observe two distinct FRET changes at low force: 1) a sharp decrease in FRET through a one-step transition, which coincides with the force-extension transition when this occurs cooperatively (Fig. 5 *E* and *F*), and 2) a gradual FRET decrease that occurs along with the noncooperative force-extension transition (Fig. 5 *G* and *H*). We stress that these alignment analyses were performed with a clear force-extension change observed for all cooperative transitions. However, for the noncooperative transitions, due to their gradual change in force extension and the noise introduced by the longer handles required for the fleezers experiments, we had to develop a different procedure that aligns the fluorescent traces (*SI Appendix*, *SI Materials and Methods*). The resulting alignment shows that the decrease in FRET is also a noncooperative process (Fig. 5*H*).

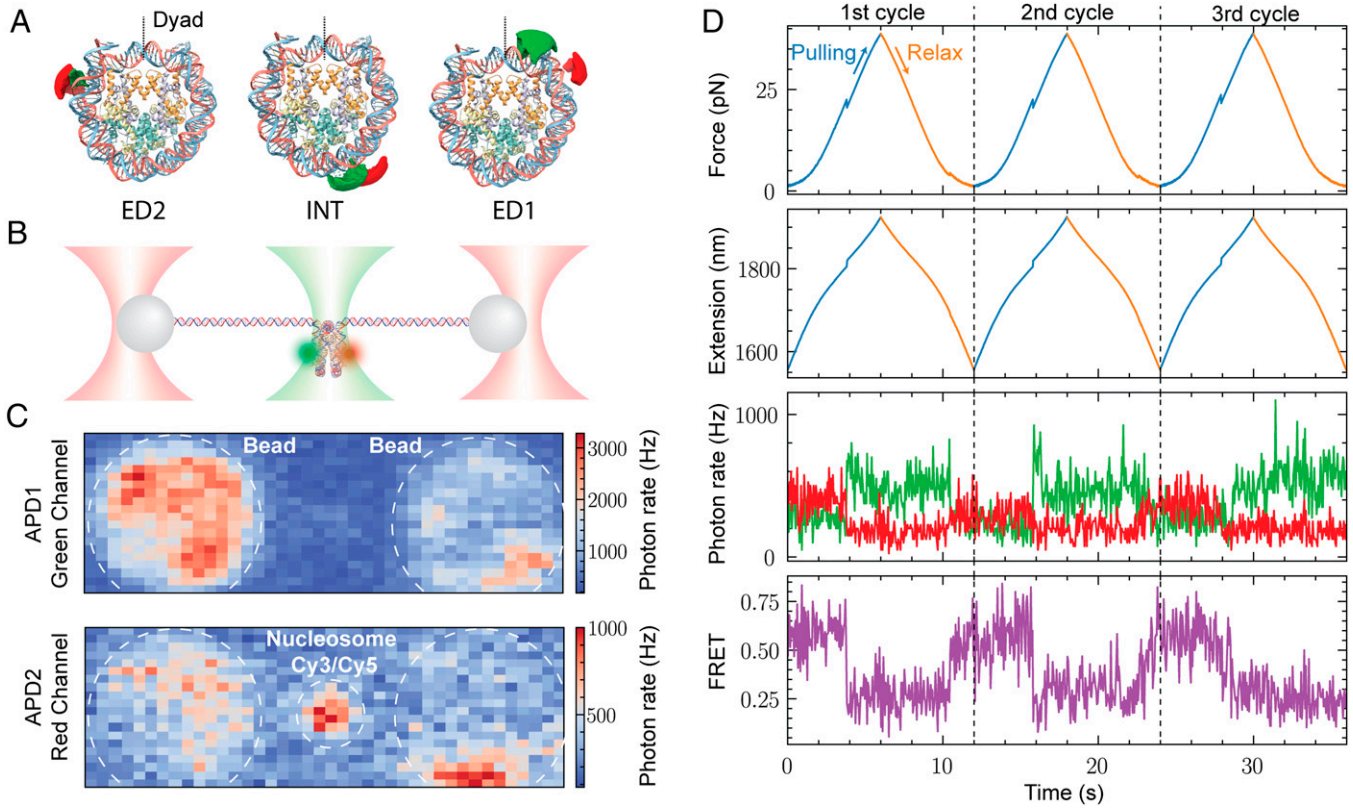

Fig. 4. Asymmetric unwrapping of Ns monitored by cotemporal force and fluorescence measurement. (*A*) Structure of N (Protein Data Bank: 6ESF), showing the position of the fluorophores Cy3 (green) and Cy5 (red) in the ED2, INT, and ED1 Ns. (*B*) Experimental geometry: single Cy3/Cy5 Ns tethered for mechanical manipulation in a fleezers setup. (*C*) Confocal scanning displaying the fluorescence of a single tethered Cy3/Cy5 N under 532-nm green laser excitation. (*D*) Simultaneous force, extension, and fluorescence measurements of ED2 N during three cycles (separated by the black dashed lines) of pulling (blue curves) and relaxation (orange curves). The fluorescence channel detects the anticorrelated changes in green and red signals corresponding to changes in FRET. Distinctive and simultaneous transitions in the force, extension, and FRET occur at high force (~20 pN) due to unwrapping events. The recovery of the FRET signal indicates N rewrapping. APD1, Avalanche photodiode 1 detector; APD2, Avalanche photodiode 2 detector.

To determine the temporal relation between the noncooperative decrease in FRET and the noncooperative change in extension in the optical tweezers channel, we compared the beginning of the noncooperative force-extension transition with the change in FRET as a function of extension (*SI Appendix, SI Materials and Methods*). Comparison of both channels shows that the FRET changes and the noncooperative force-extension transition do not occur simultaneously (Fig. 5*I*), with their separation in time varying among different molecules (*SI Appendix*, Fig. S7 *A–C*). This observation indicates the existence of a process that contributes to the change in extension in the optical tweezers channel, without involving DNA unwrapping.

To study nucleosome rewrapping, we analyzed the relaxation trajectories where high FRET was recovered (Fig. 5 *J–L*). The force-time course shows that nucleosomes rewrap most of the time in two steps and rarely in a single one at forces below ~6 pN. In the second case, it is likely that the second transition was missed due to the low force at which it occurred. While ED2 and ED1 nucleosomes can recover their FRET signals either during the first or the second zip (Fig. 5 *J* and *L*), INT nucleosomes always recover their high FRET value coincidentally with the first zip (Fig. 5*K*). Thus, although the unwrapping of nucleosomes occurs asymmetrically and sequentially starting always with the opening of the ED1 arm, the rewrapping can start with either arm in a sequential fashion.

Real-Time Observation of H2A-H2B Dimer Ejection Occurs following the High-Force Transition. As shown in Fig. 2, the mechanical disruption of nucleosomes leads to the formation of hexasomes and tetrasomes characterized by pulling trajectories, each displaying a single transition. We interpret the loss of the low-force transition as reflecting the dissociation of an H2A-H2B dimer. It is therefore of interest to establish when this dissociation occurs during the unwrapping of the nucleosome. To this end, we needed to correlate the loss of force-extension transition with heterodimer release. Accordingly, we attached a single Cy3 fluorophore via synthetic peptides to the H2A C-terminal tail (H2A-Cy3) using sortase (40, 41). This method also made it possible to purify H2A-Cy3 from the unlabeled H2A. Nucleosomes and hexasomes assembled with H2A-Cy3 were purified, and their correct integrity was confirmed by single-molecule total internal reflection fluorescence (smTIRF) microscopy (nucleosomes, *SI Appendix*, Fig. S8 *A–C*; hexasomes, *SI Appendix*, Fig. S8 *D–F*).

Next, we ligated the H2A-Cy3 nucleosomes and hexasomes to 2.5-kb DNA handles to characterize them using the fleezers instrument (*SI Appendix*, Fig. S8*G*). At low tension, we confirmed the presence of two H2A-H2B heterodimers via two-step photobleaching (*SI Appendix*, Fig. S8*H*), and the subsequent force-extension pulling trajectory exhibits the low- and high-force transitions of an intact nucleosome (*SI Appendix*, Fig. S8*I*). Similarly, tethered single hexasomes display only one-step bleaching (*SI Appendix*, Fig. S8*J*), and their force-extension pulling curves exhibit only the single high-force rip (*SI Appendix*, Fig. S8*K*). The fleezers setup yielded a lower proportion of two-step bleaching events compared to the smTIRF assay. Therefore, although two-step bleaching events for H2A-Cy3 nucleosomes were observed, single or no fluorescent events were also detected

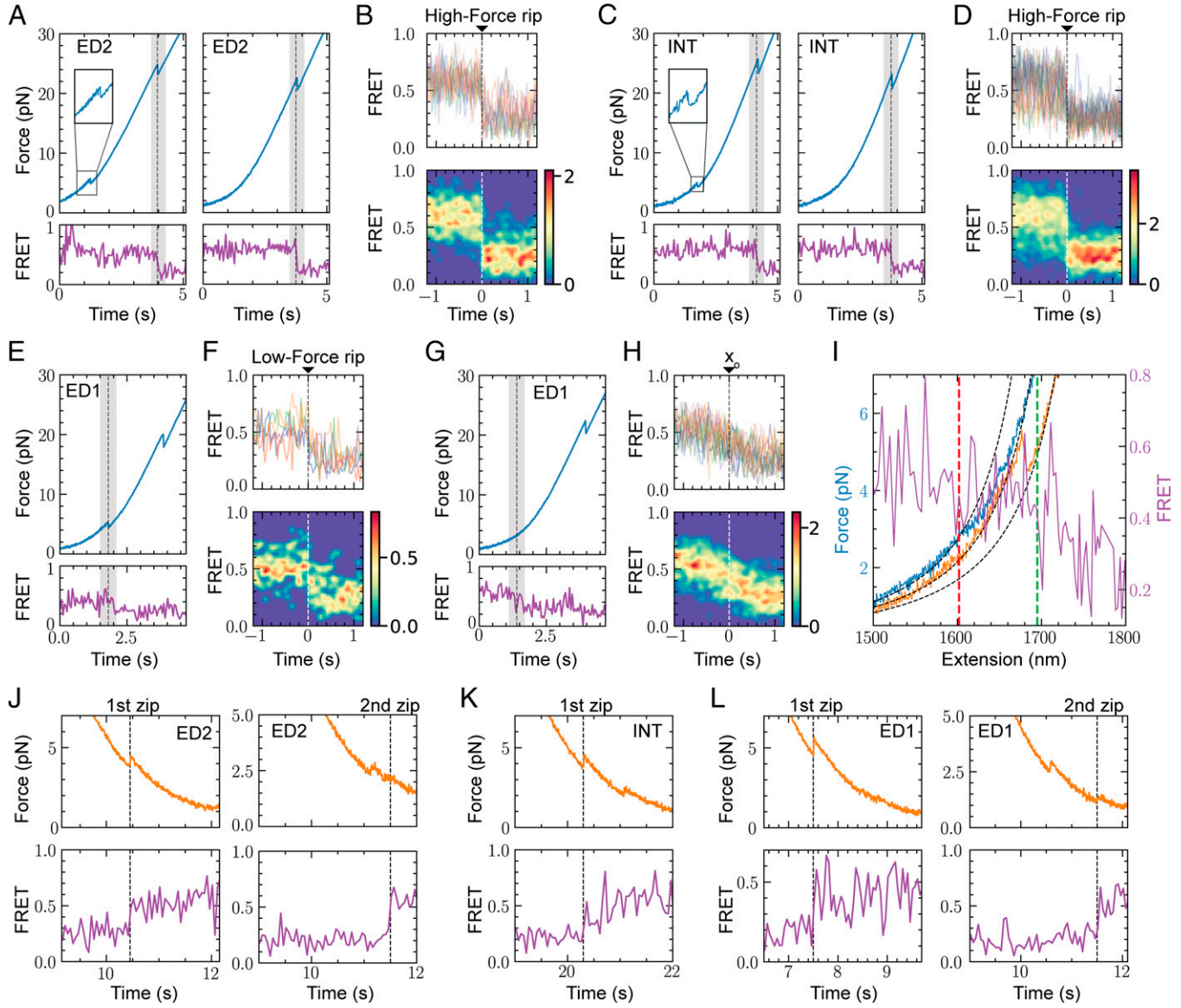

Fig. 5. Unwrapping and rewrapping trajectories of FRET Ns. Force pulling trajectory with the corresponding FRET evolution for (*A*) ED2 and (*C*) INT Ns exhibiting a cooperative (*Left*) or noncooperative (*Right*) force-extension transition at low force. The shaded gray area highlights the high-force rip. Alignment of FRET transitions for (*B*) ED2 (n = 12) and (*D*) INT (n = 23), using the high-force rip as a fiduciary mark (t = 0) (*Top*: Aligned traces; *Bottom*: 2D histogram of aligned traces). (*E*) Force pulling trajectory and FRET evolution of ED1 N exhibiting a cooperative force-extension transition at low force (gray area). (*F*) Alignment of ED1 FRET transitions (n = 5) using the cooperative low-force rip as zero time. (*G*) Force pulling trajectory and FRET evolution of ED1 N exhibiting a noncooperative force-extension transition at low force (gray area). (*H*) Alignment of ED1 FRET transitions (n = 17) exhibiting a noncooperative force-extension transition at low force (*SI Appendix*, *SI Materials and Methods*). (*I*) Temporal relation between the noncooperative decrease in FRET as a function of distance (purple trace) and the noncooperative change in extension of ED1 Ns. The fitting of the wormlike chain model (dashed black lines) to the low-force section of the N pulling curve (blue trace) exhibits a divergence as a consequence of the beginning of the noncooperative L-F (red dashed line). The start of FRET decrease is marked by the green dashed line. The H relaxation trajectory (orange curve) was included as a reference to validate the wormlike chain fitting. (*J*) ED2 N rewrapping during relaxation (orange curve) occurs in the first zip (n = 3; *Left*) or second zip (n = 3; *Right*). (*K*) INT N rewrapping occurs always in the first zip (n = 21). (*L*) ED1 N rewrapping occurs in the first zip (n = 3; *Left*) or second zip (n = 2; *Right*). The units displayed in the color maps (*B*, *D*, *F*, and *H*) correspond to the unnormalized probability density (counts).

in the fleezers instrument. We attributed this difference to photobleaching induced by the trapping laser beam (42). However, the integrity of the nucleosome can be deduced from the force-extension unwrapping trajectory, and the fluorescence signal change can inform us about the precise moment when the H2A-H2B heterodimer is lost during a pulling experiment.

The mechanical unwrapping of Cy3-labeled nucleosomes leads to the formation of hexasomes, as shown by the absence of the low-force transition in the second unwrapping trajectory (Fig. 6*A*). When does the H2A-H2B heterodimer dissociate from the histone core in the pulling/relaxation trajectories? We observed that the fluorescent signal did not change its average intensity during the unwrapping at the low-force transition (Fig. 6*B* and *SI Appendix*, Fig. S9 *A–C*), confirming that at this force regime, the nucleosome did not undergo irreversible conformational changes (17, 21). In contrast, the fluorescence suddenly drops in the region of the high-force rip (Fig. 6*B* and *SI Appendix*, Fig. S9 *A–C*). These results establish a causal relationship between the extended unwrapping of the nucleosomes occurring at the high-force transition and the loss of integrity of the histone core. Similarly, the disassembly of a hexasome with the loss of the H2A-H2B heterodimer to yield a tetrasome happens in the region of the high-force rip (*SI Appendix*, Fig. S9 *D* and *E*). To determine the temporal relationship between

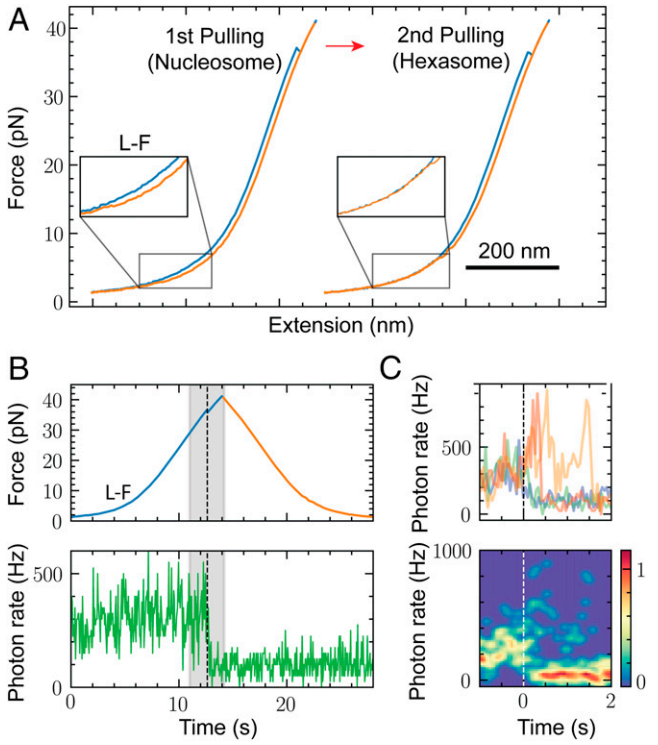

Fig. 6. Real-time detection of H2A-H2B heterodimer dissociation during N mechanical unwrapping. (*A*) H2A-Cy3 N disassembly during two cycles of pulling (blue curve) and relaxation (orange curve). The H pulling curve lacks the L-F (*Inset*). Pulling/relaxation cycles were arbitrarily shifted along the horizontal axis for illustrative purposes. (*B*) Simultaneous time course of the fluorescence and force channels during the first unwrapping/rewrapping cycle monitored in *A*. The shaded gray area indicates the regions of the H-F. (*C*) Aligned fluorescent transitions from different Ns (n = 4), using the high-force rip as a fiduciary mark (*Top*: Aligned traces; *Bottom*: 2D histogram of aligned traces).

Cy3 fluorescence loss and the high-force rip, we aligned the fluorescence of different nucleosomes relative to the time at which the force-extension transition at high force was detected in each case (Fig. 6*C*). We observed that after the high-force rip, the Cy3 fluorescence exhibits large intensity fluctuations before it drops at different time points after the rip (average delay = 113 ± 126 ms, mean and SEM).

Assignment of Changes in Extension during Mechanical Unwrapping of Nucleosomes. As shown above, we found an inconsistency between the unwrapping extension observed in the low-force transition with the optical tweezers and that reported by the cotemporal changes in FRET. Indeed, if we were to interpret the extension change of the low-force transition as purely reflecting the asymmetric unwrapping of DNA, it would correspond to ∼60 bp of DNA (20.4 nm). This extent of unwrapping should be accompanied by a loss of the FRET signal at the INT position, which is located 28 bp away from the entry point of the weak arm. However, as shown above, this FRET change only occurs during the high-force transition (Fig. 5*C*). Furthermore, the acceptor dye of the FRET pair closest to INT and used by Ngo et al. (22) (ED1.7) ceases to fluoresce at low force, and it is localized 24 bp from the entry point of the weak arm. This observation indicates that the low-force transition should correspond to the unwrapping of only ∼24 to 27 bp of DNA or about half of the outer wrap of the DNA in the crystal structure. This analysis indicates that DNA unwrapping from the histone core is not the only process contributing to the extension observed in the low-force transition with the optical tweezers. Moreover, if only ∼27 bp are unwrapped in the low-force transition, there should be ∼120 bp left partially wrapped on the nucleosome. However, the change in extension in the high-force transition (∼24.5 nm) is significantly shorter than that expected if it involves the complete unwrapping of the nucleosome as previously proposed (17, 21).

The presence of an additional process not involving unwrapping during the noncooperative low-force transition is confirmed by the change in extension detected in the optical tweezers signal before DNA unwrapping takes place, as reported by FRET (Fig. 5*I* and *SI Appendix*, Fig. S7). Such an additional process has been hypothesized in the spool model of nucleosome unwrapping, which proposes that as a consequence of its spool geometry, a nucleosome must reorient, rotate, and align when subjected to tension (21, 43, 44). However, although the spool model addresses the energetic barriers for DNA unwrapping, it did not consider the contribution of nucleosome reorientation to the observed change in extension.

We propose that at zero tension, nucleosome DNA linkers cross and emerge in opposite directions (Fig. 7, state 1). The increase in tension separates and bends the DNA linkers (Fig. 7, state 2) and causes the gradual rotation of the nucleosome (Fig. 7, state 3), marking the beginning of the noncooperative low-force transition. Once rotation has begun, ∼27 bp of DNA unwrap progressively (Fig. 7, state 4), until the nucleosome becomes aligned with the applied force (Fig. 7, state 5). To estimate the contribution of nucleosome reorientation to the observed change in extension, we developed a mechanical unwrapping model that simulates the rotational motion of a nucleosome by aligning the torque exerted at the entry and exit DNA along the pulling force direction and the unwrapping transitions (Movie S1).

Initial rotation of the nucleosome before unwrapping contributes an increase in extension of 8.1 nm (Fig. 7, state 3). At this point, an increase in end-to-end distance of ∼8.5 nm occurs, associated with the nucleosome unwrapping asymmetrically by ∼27 bp (calculated from the wormlike chain model at a force of 4 pN) plus a residual rotation of ∼3.2 nm taking place during the unwrapping (Fig. 7, states 4 and 5). This analysis yields a total change of ∼20 nm at the end of the low-force transition. When the low-force transition occurs cooperatively, the nucleosome rotation and unwrapping occur simultaneously, yielding an experimental change in extension of 20.4 ± 1.5 nm (*SI Appendix*, Table S1). When the transition occurs noncooperatively, there is a larger uncertainty in the change in extension and we obtained a value of ∼19 nm. At the end of the low-force transition, ∼120 bp remain wrapped in the nucleosome (Fig. 7, state 5).

In the high-force transition, a partially unwrapped and force-aligned nucleosome (Fig. 7, state 5) continues to rotate by ∼180° (45) as it further unwraps (and therefore the rotation does not contribute to a change in extension. Fig. 7, state 6) to yield an experimental change in extension of 24.5 ± 1.6 nm in a single step (*SI Appendix*, Table S2). The sharp drop in FRET at the entry (ED2) and exit (INT) DNA points coincides with the rip (Fig. 5 *A*–*D*), indicating that unlike what is observed at low force, DNA unwraps from both ends simultaneously during the high-force transition. Using our mechanical unwrapping model, the ∼24.5-nm change in extension observed in the high-force transition corresponds to the unwrapping of ∼76 bp of DNA (Movie S1). Accordingly, ∼43 bp remained wrapped at the end of the high-force transition (Fig. 7, state 7). Because state 7 compared to bare DNA is similar to the change in extension between hexasomes and nucleosomes (Fig. 2*E*), we

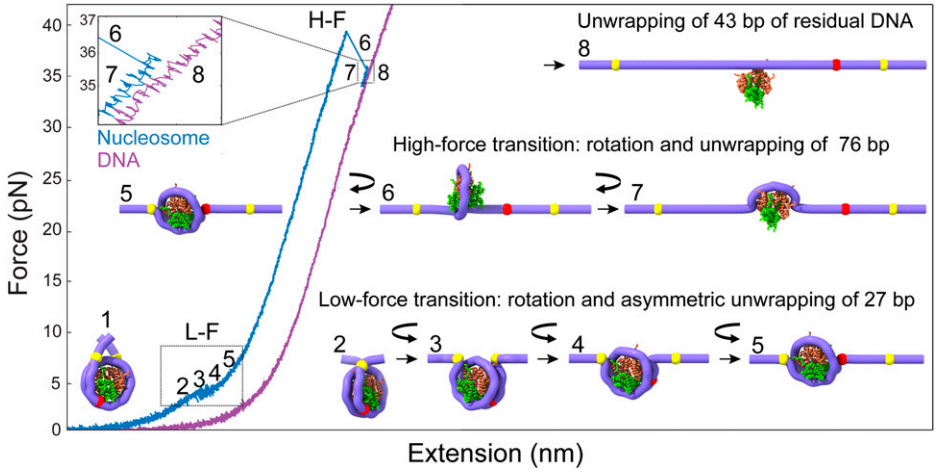

Fig. 7. Annotation of the structural changes corresponding to the force-extension transitions during the mechanical unwrapping of N. Upon the application of the external force, the N arms at zero force (state 1) align along the pulling axis (state 2). During the noncooperative L-F (~4 pN; states 2 to 5), the N first rotates (curved arrow; states 2 to 3) without unwrapping, keeping the DNA entry and exit points in contact with the core particle (yellow marks). Then, the N continues to rotate while the DNA begins to unwrap asymmetrically and progressively by ~27 bp (red mark), corresponding to the detachment of the distal or weak DNA arm (states 3 to 5). This last conformation (state 5) is maintained along the pulling curve until it reaches the H-F. During the H-F, N rotates ~180° in the opposite direction of the first rotation, and ~76 bp are unwrapped in a single step observed as a rip (states 6 to 7). At the end of the H-F, ~43 bp remained wrapped at the histone core. Around 13 bp are further unwrapped noncooperatively at the end of the H-F, leaving about 30 bp wrapped around the N, which are experimentally observed as the difference in extension (*Top Left Inset*) between the unwrapped N (blue force-extension curve) and bare DNA (state 8; purple force-extension curve).

propose that this state is stable because the heterodimer stabilizes the tetrasome structure. In the case of tetrasomes, the lack of a dimer leads to the overlap of the tetrasome pulling curve with the DNA pulling curve Fig. 2*E*, despite the tetramer still being bound to the DNA.

This analysis predicts that a difference in end-to-end distance of 6.2 nm should be observed between the nucleosome at the end of the high-force transition and a bare DNA molecule of the same total length (Fig. 7, state 8 and Movie S1). In support of the mechanical unwrapping model, we developed a geometrical model of nucleosome unwrapping which treats the nucleosome as a spherical particle (*SI Appendix*, Fig. S10 and *SI Materials and Methods* for details). Applying this model to the high-force transition, we determined that the 24.5 nm of change in extension observed during the high-force transition should correspond to ~74 ± 5 bp of DNA, in close agreement with the mechanical unwrapping model. However, experimentally, we observe a difference in end-to-end distance between the nucleosome pulling curve after the high-force transition and the corresponding pulling curve of bare DNA of ~2.3 nm (Fig. 2*E*). Using the geometrical model, we estimate that this difference in extension should correspond to 30 ± 3 bp remaining wrapped (not 43 bp) after the high-force transition. Thus, we propose that during or after the high-force transition, 13 ± 3 bp unwrap noncooperatively, a process not directly resolvable with our methodology. Interestingly, 30 bp distributed symmetrically around the dyad have been experimentally determined to be the strongest region of histone-DNA interaction (46).

A similar analysis indicates that the hexasome does not display a low-force transition because one of its arms has been unwrapped, and the resulting structure is aligned so that the application of force does not generate a change in extension due to rotation. In the case of the tetrasome, the remaining difference of ~6 nm with respect to bare DNA (Fig. 2*E*) indicates that ~40 bp remain wrapped at the end of the low-force transition, which must involve the unwrapping of ~30 bp and a contribution due to rotation.

Discussion

Although mechanical manipulation of nucleosomes has been studied for around 20 y, the elucidation of the molecular changes occurring during unwrapping and rewrapping remained controversial. Using FRET in a cotemporal fashion with optical tweezers, we have been able to assign the observed force-extension transitions to the unwrapping and rewrapping of specific regions in the nucleosome. We find that during unwrapping, nucleosomes can disassemble stochastically into hexasomes and tetrasomes, whose force-extension trajectories we establish. We propose a model of nucleosome unwrapping that explains previous discrepancies related to the directionality and extension of DNA unwrapping (17, 21, 22). Furthermore, we show that the assignment of the changes in extension accompanying the unwrapping transitions must include the contribution of the force-induced rotation of the nucleosome as it unwraps.

As previously determined, the entry and exit arms of the 601 NPS possess different mechanical flexibilities, which results in the asymmetric unwrapping of the two arms (22). The wrapping of the DNA around the histone core is energetically costly due to the large persistence length of DNA (~50 nm). This cost must be paid by the binding energy between the DNA and the histones. The mechanically stiffer segment corresponds to the DNA weak arm because more of its binding energy to the histones must be used relative to the strong arm to wrap it around the core. As a result, the weak arm unwraps first under mechanical manipulation. Accordingly, the asymmetric unwrapping results from both the differential flexibilities of the DNA arms and their interactions with the histone core. When DNA sequence flexibility is symmetrized, either arm can then open before the other because under tension, the unwrapping involves the thermally induced crossing of a barrier, a stochastic process. It has been shown that once one of the arms opens, conformational change and structural reaccommodation of the nucleosome take place. Indeed, once the ED1 arm unwraps, it triggers conformational changes in different regions of the octamer that bring into closer proximity the opposite ED2 arm and mechanically stabilizes it (47).

The unwrapping of a nucleosome arm at low forces indicates that the interactions involved in maintaining its wrapped structure are relatively weak, consistent with findings from single-molecule unzipping experiments (46). Recently, molecular dynamic simulations identified a region in H3 known as the H3 latch that, in combination with its N-terminal tail, interacts with both the inner and outer DNA wrap, stabilizing the DNA arm at the superhelical location (SHL) +7 and keeping it wrapped (48). The limited extent of the low-force transition (~27 bp) probably reflects the strength of the subsequent interactions, involving those between the α1 helices and tails of H2A and H2B with the SHL ±4 and with the SHL ±5 (where the INT FRET pair is located; *SI Appendix*, Fig. S11 *A* and *B*). These regions exhibit a local concentration of positive charges that interact with the negative backbone of the DNA, as revealed by calculations of the nucleosome electrostatic surface potential using the Poisson-Boltzmann equation (*SI Appendix*, Fig. S11 *C* and *D*) (49).

Our observation of a high-force transition confirms the fact that when one of the outer arms of the nucleosome is unwrapped at forces below 5 pN (low-force transition), the remaining nucleosome structure rearranges, and the interaction of the opposite arm with the histone core is energetically stabilized so that it will only unwrap at a mean force above 25 pN (high-force transition). This interpretation also explains the unwrapping trajectory of the hexasome: removal of one heterodimer is similar (but not identical) to the mechanical opening of one arm of the nucleosome. The loss of the dimer leads to the stabilization of the DNA arm wrapped around the remaining heterodimer. As a result, the hexasome trajectory lacks the low-force transition and displays only a high-force transition somewhat weakened relative to that of the nucleosome trajectory (occurring at a mean force of ~25 pN instead of ~30 pN, respectively; Fig. 2 *B* and *E*). Part of the reaccommodation and stabilization of the nucleosome harboring an unwrapped arm or of the hexasome missing a heterodimer could originate in a reduced electrostatic repulsion between wrapped DNA segments in the nucleosome that accompanies the first unwrapping event (43). When at this high force, the most external points of contact between the DNA and the histone finally rupture; most interactions following those points are then unable to contain the propagation of the unwrapping front, which give rise to the cooperative nature of the high-force transition. At this point, only interactions between SHL ±1 and SHL ±2 with α1 helices and tails of H4 and H3 remain (*SI Appendix*, Fig. S11).

We find that while the unwrapping process is asymmetric and starts at the weak nucleosomal DNA arm, the rewrapping always starts at the INT segment, followed nonpreferentially by either the weak or the strong arm (Fig. 5 *J* and *L*). However, the rewrapped nucleosome recovers its unwrapping asymmetry in the next pulling cycle (Fig. 4*D* and *SI Appendix*, Fig. S6).

It has been shown that RNA polymerase II (Pol II) is not strong enough to separate the DNA wrapped around the nucleosome. Instead, it advances through the nucleosome by rectifying the fluctuations of the DNA off the histone octamer (50). Structural and biochemical studies have shown that Pol II transcription exhibits major pauses at nucleosomal positions SHL ±5 and SHL ±1 independent of the nucleosomal arm from which transcription started (51–53). Taken together, these observations can be rationalized in the context of our nucleosome unwrapping model involving the low- and high-force transitions. First, Pol II exhibits a weak pause at SHL −7 and awaits spontaneous fluctuations that unwrap ~27 bp of DNA (low-force transition), allowing Pol II entry into the nucleosome until it reaches SHL −5. Second, Pol II paused at the SHL −5 awaits larger thermal fluctuations to overcome strong histone-DNA interactions associated with the high-force transition, thus constituting a major pausing site. We note that it is possible that the forces needed to break up these interactions by thermal fluctuations are lower compared to the forces estimated in our experiments due to our pulling geometry (44, 45) and the bulkiness of Pol II. During transcription, which allows invasion of SHL −1 without breaking the interactions of the distal heterodimer with SHL +5 (52, 53), these interactions are not broken at the same time.

DNA unwrapping at the low-force transition partially exposes one H2A-H2B heterodimer but does not lead to its dissociation, as confirmed by our fleezers assay (Fig. 6) and further supported by 1) the reversible nature of the low-force transition (17, 21), 2) the structure of the partially unwrapped (~25 to 30 bp) nucleosomes observed by cryo-electron microscopy (cryo-EM) (47), and 3) the exposed H2A-H2B heterodimer observed by cryo-EM in nucleosomal transcription complexes stalled at SHL −5 (52, 53). Our experiments show, however, that H2A-H2B heterodimer dissociation can occur after the high-force transition, in which several DNA-histone interactions are broken. These contacts are partially electrostatic, as indicated by the decrease in the rupture force observed with increasing ionic strength (*SI Appendix*, Table S2). This result is in agreement with single-molecule FRET measurements of salt-induced nucleosome disassembly showing that H2A-H2B dimer dissociation requires extensive DNA unwrapping (54). Furthermore, the rupture of interactions between H2A-H2B and SHL +5 is required for the loss of the heterodimer but not sufficient. Indeed, we note that after the first pulling and relaxation cycle, hexasomes or tetrasomes are generated only ~28% of the time in each case, while the nucleosome retains its integrity in the remaining 40% (*SI Appendix*, Table S3). These observations suggest that histone-histone interactions can preserve the H2A-H2B heterodimer attached to the histone core after DNA unwrapping. Although it remains unclear in our assay which one of the two H2A-H2B heterodimers (proximal or distal) is dissociated during the high-force transition, we speculate that the distal heterodimer (associated with the more rigid ED1 DNA arm) is the first to dissociate based on the preferential assembly of hexasomes containing this proximal heterodimer (55, 56).

In summary, we identify the DNA regions involved with each transition observed in the mechanical unwrapping/rewrapping trajectories of nucleosomes, as well as of the hexasomes, and tetrasomes generated during the stochastic disassembly of the former. The characterization of their mechanical properties will make it possible to identify the subnucleosomal particles generated by the action of polymerases, remodelers, and histone chaperones in future force spectroscopy studies.

Materials and Methods

Protein Expression and Purification. Recombinant *X. laevis*, human, and yeast histones H2A, H2B, H3, and H4 were expressed in *Escherichia coli* BL21(DE3) and purified from inclusion bodies as previously described (57). Recombinant His-tagged sortase 5M in the pET30b vector was purified as previously described with some modifications (58).

Synthesis of Fluorescently Labeled 601 NPS. ED1, INT, and ED2 fluorescent DNA templates were generated by PCR. The primers used are based on published work (22), and Cy3-NHS and Cy5-NHS (Lumiprobe) were conjugated to the forward and reverse primers, respectively. Labeled primers were used to amplify the 601 NPS from the PGEM 601 vector.

Data Availability. The change in extension analysis code and the mechanical unwrapping model code have been deposited in GitHub (https://github.com/CesarDiazCelis1/Nucleosome-Unwrapping) (59). The optical tweezers data are available via Zenodo (https://doi.org/10.5281/zenodo.6780532) (60). Materials used in this research are available on request from C.B. All other study data are included in the article and/or supporting information.

ACKNOWLEDGMENTS. We thank Professor Geeta Narlikar for providing the expression vectors of *X. laevis* histones. We thank Dr. Simon Pöpsel and Professor Eva Nogales for their help with preparative electrophoresis purification. This research was supported by the Nanomachine program (KC1203) funded by the Office of Basic Energy Sciences of the U.S. Department of Energy (contract DE-AC02-05CH11231 to C.B.) and by the NIH (grant R01GM032543). C.B. is a Howard Hughes Medical Institute Investigator.

Author affiliations: [a]Jason L. Choy Laboratory of Single-Molecule Biophysics, University of California, Berkeley, CA 94720; [b]California Institute for Quantitative Biosciences, University of California, Berkeley, CA 94720; [c]HHMI, University of California, Berkeley, CA 94720; [d]Department of Chemistry, University of California, Berkeley, CA 94720; [e]Biophysics Graduate Group, University of California, Berkeley, CA 94720; [f]Applied Science and Technology Graduate Group, University of California, Berkeley, CA 94720; [g]The Molecular Foundry, Lawrence Berkeley National Laboratory, Berkeley, CA 94720; [h]Physics Graduate Group, University of California, Berkeley, CA 94720; [i]Department of Physics, University of California, Berkeley, CA 94720; [j]Department of Molecular and Cell Biology, University of California, Berkeley, CA 94720; [k]Molecular Biophysics and Integrative Bioimaging Division, Lawrence Berkeley National Laboratory, Berkeley, CA 94720; and [l]Kavli Energy Nanoscience Institute, University of California, Berkeley, CA 94720

Author contributions: C.D.-C., C.C.-C., R.P.S., and C.B. designed research; C.D.-C., C.C.-C., R.P.S., J.P.C., M.Z., E.C., A.Q.C., M.V., J.K., and B.O. performed research; C.B. contributed new reagents/analytic tools; C.D.-C., C.C.-C., R.P.S., J.P.C., M.Z., and B.O. analyzed data; and C.D.-C., C.C.-C., R.P.S., J.P.C., and C.B. wrote the paper.

1. R. D. Kornberg, Chromatin structure: A repeating unit of histones and DNA. *Science* **184**, 868–871 (1974).
2. K. Luger, A. W. Mäder, R. K. Richmond, D. F. Sargent, T. J. Richmond, Crystal structure of the nucleosome core particle at 2.8 A resolution. *Nature* **389**, 251–260 (1997).
3. S. K. Williams, D. Truong, J. K. Tyler, Acetylation in the globular core of histone H3 on lysine-56 promotes chromatin disassembly during transcriptional activation. *Proc. Natl. Acad. Sci. U.S.A.* **105**, 9000–9005 (2008).
4. Z. Wen, L. Zhang, H. Ruan, G. Li, Histone variant H2A.Z regulates nucleosome unwrapping and CTCF binding in mouse ES cells. *Nucleic Acids Res.* **48**, 5939–5952 (2020).
5. C. R. Brown, C. Mao, E. Falkovskaia, J. K. Law, H. Boeger, In vivo role for the chromatin-remodeling enzyme SWI/SNF in the removal of promoter nucleosomes by disassembly rather than sliding. *J. Biol. Chem.* **286**, 40556–40565 (2011).
6. T. Wang *et al.*, The histone chaperone FACT modulates nucleosome structure by tethering its components. *Life Sci. Alliance* **1**, e201800107 (2018).
7. G. Sirinakis *et al.*, The RSC chromatin remodelling ATPase translocates DNA with high force and small step size. *EMBO J.* **30**, 2364–2372 (2011).
8. S. S. Teves, S. Henikoff, Transcription-generated torsional stress destabilizes nucleosomes. *Nat. Struct. Mol. Biol.* **21**, 88–94 (2014).
9. V. Böhm *et al.*, Nucleosome accessibility governed by the dimer/tetramer interface. *Nucleic Acids Res.* **39**, 3093–3102 (2011).
10. Y. Chen *et al.*, Asymmetric unwrapping of nucleosomal DNA propagates asymmetric opening and dissociation of the histone core. *Proc. Natl. Acad. Sci. U.S.A.* **114**, 334–339 (2017).
11. Y. Chen *et al.*, Revealing transient structures of nucleosomes as DNA unwinds. *Nucleic Acids Res.* **42**, 8767–8776 (2014).
12. A. Gansen *et al.*, Nucleosome disassembly intermediates characterized by single-molecule FRET. *Proc. Natl. Acad. Sci. U.S.A.* **106**, 15308–15313 (2009).
13. I. Oohara, A. Wada, Spectroscopic studies on histone-DNA interactions. II. Three transitions in nucleosomes resolved by salt-titration. *J. Mol. Biol.* **196**, 399–411 (1987).
14. Y. Cui, C. Bustamante, Pulling a single chromatin fiber reveals the forces that maintain its higher-order structure. *Proc. Natl. Acad. Sci. U.S.A.* **97**, 127–132 (2000).
15. M. L. Bennink *et al.*, Unfolding individual nucleosomes by stretching single chromatin fibers with optical tweezers. *Nat. Struct. Biol.* **8**, 606–610 (2001).
16. B. Brower-Toland *et al.*, Specific contributions of histone tails and their acetylation to the mechanical stability of nucleosomes. *J. Mol. Biol.* **346**, 135–146 (2005).
17. B. D. Brower-Toland *et al.*, Mechanical disruption of individual nucleosomes reveals a reversible multistage release of DNA. *Proc. Natl. Acad. Sci. U.S.A.* **99**, 1960–1965 (2002).
18. M. Kruithof *et al.*, Single-molecule force spectroscopy reveals a highly compliant helical folding for the 30-nm chromatin fiber. *Nat. Struct. Mol. Biol.* **16**, 534–540 (2009).
19. M. Simon *et al.*, Histone fold modifications control nucleosome unwrapping and disassembly. *Proc. Natl. Acad. Sci. U.S.A.* **108**, 12711–12716 (2011).
20. C. Claudet, D. Angelov, P. Bouvet, S. Dimitrov, J. Bednar, Histone octamer instability under single molecule experiment conditions. *J. Biol. Chem.* **280**, 19958–19965 (2005).
21. S. Mihardja, A. J. Spakowitz, Y. Zhang, C. Bustamante, Effect of force on mononucleosomal dynamics. *Proc. Natl. Acad. Sci. U.S.A.* **103**, 15871–15876 (2006).
22. T. T. Ngo, Q. Zhang, R. Zhou, J. G. Yodh, T. Ha, Asymmetric unwrapping of nucleosomes under tension directed by DNA local flexibility. *Cell* **160**, 1135–1144 (2015).
23. M. Kruithof, J. van Noort, Hidden Markov analysis of nucleosome unwrapping under force. *Biophys. J.* **96**, 3708–3715 (2009).
24. P. Chen *et al.*, Functions of FACT in breaking the nucleosome and maintaining its integrity at the single-nucleosome level. *Mol. Cell* **71**, 284–293.e4 (2018).
25. P. Gupta, J. Zlatanova, M. Tomschik, Nucleosome assembly depends on the torsion in the DNA molecule: A magnetic tweezers study. *Biophys. J.* **97**, 3150–3157 (2009).
26. R. Vlijm *et al.*, Nucleosome assembly dynamics involve spontaneous fluctuations in the handedness of tetrasomes. *Cell Rep.* **10**, 216–225 (2015).
27. M. Y. Sheinin, M. Li, M. Soltani, K. Luger, M. D. Wang, Torque modulates nucleosome stability and facilitates H2A/H2B dimer loss. *Nat. Commun.* **4**, 2579 (2013).
28. P. T. Lowary, J. Widom, New DNA sequence rules for high affinity binding to histone octamer and sequence-directed nucleosome positioning. *J. Mol. Biol.* **276**, 19–42 (1998).
29. K. Tóth *et al.*, Histone- and DNA sequence-dependent stability of nucleosomes studied by single-pair FRET. *Cytometry A* **83**, 839–846 (2013).
30. R. T. Simpson, D. W. Stafford, Structural features of a phased nucleosome core particle. *Proc. Natl. Acad. Sci. U.S.A.* **80**, 51–55 (1983).
31. K. K. Sinha, J. D. Gross, G. J. Narlikar, Distortion of histone octamer core promotes nucleosome mobilization by a chromatin remodeler. *Science* **355**, eaaa3761 (2017).
32. A. Gansen *et al.*, High precision FRET studies reveal reversible transitions in nucleosomes between microseconds and minutes. *Nat. Commun.* **9**, 4628 (2018).
33. T. Moss, R. M. Stephens, C. Crane-Robinson, E. M. Bradbury, A nucleosome-like structure containing DNA and the arginine-rich histones H3 and H4. *Nucleic Acids Res.* **4**, 2477–2485 (1977).
34. R. H. Simon, R. D. Camerini-Otero, G. Felsenfeld, An octamer of histones H3 and H4 forms a compact complex with DNA of nucleosome size. *Nucleic Acids Res.* **5**, 4805–4818 (1978).
35. T. Zou *et al.*, Direct observation of H3-H4 octasome by high-speed AFM. *Chemistry* **24**, 15998–16002 (2018).
36. M. J. Comstock, T. Ha, Y. R. Chemla, Ultrahigh-resolution optical trap with single-fluorophore sensitivity. *Nat. Methods* **8**, 335–340 (2011).
37. K. D. Whitley, M. J. Comstock, Y. R. Chemla, High-resolution optical tweezers combined with single-molecule confocal microscopy. *Methods Enzymol.* **582**, 137–169 (2017).
38. V. P. Desai *et al.*, Co-temporal force and fluorescence measurements reveal a ribosomal gear shift mechanism of translation regulation by structured mRNAs. *Mol. Cell* **75**, 1007–1019.e5 (2019).
39. T. T. Ngo, T. Ha, Nucleosomes undergo slow spontaneous gaping. *Nucleic Acids Res.* **43**, 3964–3971 (2015).
40. I. Chen, B. M. Dorr, D. R. Liu, A general strategy for the evolution of bond-forming enzymes using yeast display. *Proc. Natl. Acad. Sci. U.S.A.* **108**, 11399–11404 (2011).
41. B. M. Dorr, H. O. Ham, C. An, E. L. Chaikof, D. R. Liu, Reprogramming the specificity of sortase enzymes. *Proc. Natl. Acad. Sci. U.S.A.* **111**, 13343–13348 (2014).
42. M. P. Landry, P. M. McCall, Z. Qi, Y. R. Chemla, Characterization of photoactivated singlet oxygen damage in single-molecule optical trap experiments. *Biophys. J.* **97**, 2128–2136 (2009).
43. I. M. Kulić, H. Schiessel, DNA spools under tension. *Phys. Rev. Lett.* **92**, 228101 (2004).
44. B. Sudhanshu *et al.*, Tension-dependent structural deformation alters single-molecule transition kinetics. *Proc. Natl. Acad. Sci. U.S.A.* **108**, 1885–1890 (2011).
45. G. Reddy, D. Thirumalai, Asymmetry in histone rotation in forced unwrapping and force quench rewrapping in a nucleosome. *Nucleic Acids Res.* **49**, 4907–4918 (2021).
46. M. A. Hall *et al.*, High-resolution dynamic mapping of histone-DNA interactions in a nucleosome. *Nat. Struct. Mol. Biol.* **16**, 124–129 (2009).
47. S. Bilokapic, M. Strauss, M. Halic, Histone octamer rearranges to adapt to DNA unwrapping. *Nat. Struct. Mol. Biol.* **25**, 101–108 (2018).
48. G. A. Armeev, A. S. Kniazeva, G. A. Komarova, M. P. Kirpichnikov, A. K. Shaytan, Histone dynamics mediate DNA unwrapping and sliding in nucleosomes. *Nat. Commun.* **12**, 2387 (2021).
49. M. Gebala, S. L. Johnson, G. J. Narlikar, D. Herschlag, Ion counting demonstrates a high electrostatic field generated by the nucleosome. *eLife* **8**, e44993 (2019).
50. C. Hodges, L. Bintu, L. Lubkowska, M. Kashlev, C. Bustamante, Nucleosomal fluctuations govern the transcription dynamics of RNA polymerase II. *Science* **325**, 626–628 (2009).
51. V. A. Bondarenko *et al.*, Nucleosomes can form a polar barrier to transcript elongation by RNA polymerase II. *Mol. Cell* **24**, 469–479 (2006).
52. H. Ehara *et al.*, Structural insight into nucleosome transcription by RNA polymerase II with elongation factors. *Science* **363**, 744–747 (2019).
53. T. Kujirai *et al.*, Structural basis of the nucleosome transition during RNA polymerase II passage. *Science* **362**, 595–598 (2018).
54. J. Lee, T. H. Lee, Single-molecule investigations on histone H2A-H2B dynamics in the nucleosome. *Biochemistry* **56**, 977–985 (2017).
55. R. F. Levendosky, A. Sabantsev, S. Deindl, G. D. Bowman, The Chd1 chromatin remodeler shifts hexasomes unidirectionally. *eLife* **5**, e21356 (2016).
56. Y. Arimura, H. Tachiwana, T. Oda, M. Sato, H. Kurumizaka, Structural analysis of the hexasome, lacking one histone H2A/H2B dimer from the conventional nucleosome. *Biochemistry* **51**, 3302–3309 (2012).
57. J. Wittmeyer, A. Saha, B. Cairns, DNA translocation and nucleosome remodeling assays by the RSC chromatin remodeling complex. *Methods Enzymol.* **377**, 322–343 (2004).
58. H. Hirakawa, S. Ishikawa, T. Nagamune, Design of Ca^{2+}-independent *Staphylococcus aureus* sortase A mutants. *Biotechnol. Bioeng.* **109**, 2955–2961 (2012).
59. C. Díaz-Celis *et al.*, Assignment of structural transitions during mechanical unwrapping of nucleosomes and their disassembly products. GitHub. https://github.com/CesarDiazCelis1/Nucleosome-Unwrapping. Accessed 29 June 2022.
60. C. Díaz-Celis *et al.*, Assignment of structural transitions during mechanical unwrapping of nucleosomes and their disassembly products. Zenodo. https://doi.org/10.5281/zenodo.6780532. Accessed 29 June 2022.